Quantitative Analysis of Myocardial Kinetics of 15-*p*-[Iodine-125] Iodophenylpentadecanoic Acid

Timothy R. DeGrado*, James E. Holden, Chin K. Ng, David M. Raffel, and S. John Gatley

Department of Medical Physics, 1530 Medical Sciences Center, University of Wisconsin, Madison, Wisconsin; and Franklin-McLean Institute, University of Chicago, Illinois

Myocardial extraction and the characteristic tissue clearance of radioactivity following bolus injections of a radioiodinated (^{125}I) long chain fatty acid (LCFA) analog 15-p-iodophenylpentadecanoic acid (IPPA) were examined in the isolated perfused working rat heart. Radioactivity remaining in the heart was monitored with external scintillation probes. A compartmental model which included nonesterified tracer, catabolite, and complex lipid compartments successfully fitted tissue time-radioactivity residue curves, and gave a value for the rate of IPPA oxidation 1.8 times that obtained from steady-state release of tritiated water from labeled palmitic acid. The technique was sensitive to the impairment of LCFA oxidation in hearts of animals treated with the carnitine palmitoyltransferase I inhibitor, 2[5(4-chlorophenyl)pentyl]oxirane-2-carboxylate (POCA). IPPA or similar modified fatty acids may be better than ^{11}C-labeled physiological fatty acids such as palmitate in this type of study, because efflux of unoxidized tracer and catabolite(s) from the heart are kinetically more distinct, and their contributions to the early data can be reliably separated. This technique may be suitable for extension to in vivo measurements with position tomography and appropriate modified fatty acids.

J Nucl Med 30:1211–1218, 1989

The noninvasive assessment of myocardial utilization of exogenous long chain fatty acids (LCFA) has been proposed using radiolabeled long chain fatty acids (*1–5*). Because the clearance of radiolabel from the myocardium is generally biphasic following bolus administration of tracer, the measured time-radioactivity curves (residue curves) have been analyzed in terms of the sum of two exponential components. The more rapid component has been interpreted as washout of radiolabeled catabolite from the rapid oxidation of a fraction of the tracer, while the slower component reflects turnover of label incorporated into complex lipids. Quantitative analysis of the residue curves has thus far been limited to such biexponential fitting, or "curve-peeling" (*1*).

Recent biochemical and kinetic investigations with [1-^{11}C]palmitic acid (CPA) (*2,3,6,7*) and ^{123}I-17-iodoheptadecanoic acid (IHPA) (*8,9*) in myocardium have revealed a primary limitation of curve-peeling. What appears to be one component in the early clearance phase actually represents two or more clearance processes. The relative size and the fractional clearance rate, or slope, of the early phase are dependent not only on the diffusion of labeled catabolite(s) but also on the backdiffusion of unoxidized tracer. This has been shown to be the case with CPA, as both labeled CO_2 and CPA clear the heart at all times and the proportion of each in the washout is time-dependent (*2,6,7*). Thus, the residue curve during the early oxidative phase is strongly influenced by backdiffusion of nonesterified tracer and this influence cannot be kinetically discriminated by exponential fitting. In ischemic myocardium, unidirectional extraction of palmitate analogs was found to be relatively constant while backdiffusion is increased (*3,5–7*), reflecting decreased net utilization rates of LCFA. A successful radiotracer technique must be able to account for the variable backdiffusion component.

Received June 29, 1988; revision accepted Mar. 17, 1989.

For reprints contact: James E. Holden, PhD, 1530 Medical Sciences Center, 1300 University Ave., Madison, WI 53706.

* Present address: Institut für Chemie 1, Kernforschungsanlage Jülich GmbH, Postfach 1913, D-5170 Jülich, FRG.

As promising alternatives to curve-peeling, quantitative analyses of LCFA kinetics using compartmental modeling techniques have been advanced. In studies with CPA in canine heart, Huang et al. (*10*) found that a three-compartment model including nonesterified CPA, complex lipid, and labeled CO_2 successfully fitted tissue residue curves, although estimates of LCFA oxidation were consistently greater than directly measured values. Dubois et al. (*11*) and Bontemps et al. (*12*) used similar techniques to fit residue curves of ^{123}I-16-iodo-9-hexadecenoic acid (IHA) in the Langendorff perfused rat heart. Changes in the metabolism of IHA induced by alteration of substrate or impairment of fatty acid oxidation by the carnitine palmitoyltransferase I inhibitor, 2[5(4-chlorophenyl)pentyl]oxirane-2-carboxylate (POCA) were reliably indicated by compartmental modeling. However, backdiffusion of nonesterified IHA was not included in that model since albumin was not added to the perfusion medium.

An isolated working rat heart system has been developed in this laboratory to model tomographically isolated volumes of myocardial tissue. This system allows the external measurement of radioactivity in the heart from positron-emitting isotopes as well as low-energy, single photon emitters such as iodine-125 (^{125}I). The heart is isolated from other tissues, allowing for control of substrates and hormones in the perfusion medium and manipulation of mechanical workload. Also, a variety of useful radiotracer and biochemical techniques are made available. The metabolic pathways for radiotracers are found by identification of labeled metabolites in coronary effluent and tissue. Recently, we have investigated the metabolism and kinetics of ^{125}I-16-iodohexadecanoic acid (IHDA) and ^{125}I-15(p-iodophenyl)pentadecanoic acid (IPPA) in working rat hearts perfused with medium containing fatty acids and albumin (*13*). These LCFA analogs appeared suitable for compartmental analysis because the diffusion rates of their principal catabolites were significantly slower than backdiffusion of unoxidized tracer from hearts. Furthermore, the appearance of the residue curves and the patterns of radioactive compounds in heart homogenates and in the coronary effluent were reproducibly altered by pretreatment of animals with POCA. In the present study we aimed to evaluate the usefulness of the compartmental modeling approach, and to investigate the effects of inhibition of LCFA oxidation with POCA on calculated compartmental fluxes in the myocardium using IPPA.

METHODS

General

Male Sprague-Dawley rats (200-250g) fed ad libitum were used. The preparation and formulation of [^{125}I]IPPA; isolation and perfusion of working rat hearts (15 cm H_2O preload, 130 cm H_2O afterload), the gamma-radiation detection system, and the rapid arterial arterial bolus administration of IPPA have been previously described (*13*). All hearts were perfused with Krebs-Henseleit buffer containing 0.15 m*M* palmitate-albumin and 5 m*M* glucose. When required, rats were injected intraperitoneally with 30 mg/kg POCA in distilled water 3-4 hr before excision of hearts. In the present study, four hearts were studied without pretreatment (control) and four hearts with pretreatment (POCA).

An index of palmitate oxidation was estimated from the rate of ^3H_2O production in hearts perfused with palmitate-albumin medium containing ~60 μCi/l [9,10-^{3}H]palmitic acid (^{3}H-PA) (NEN Research Products, Boston, MA). ^3H_2O was separated from ^{3}H-PA in coronary effluent samples by precipitation of ^{3}H-PA-albumin with acid. Each 1-ml sample was pipetted into an Eppendorff microcentrifuge tube containing 0.25 ml of 15% perchloric acid and vortexed for 5 sec. After 2 min of centrifugation, the supernatant fraction was removed. The pellet was rinsed with 0.75 ml 3% perchloric acid, vortexed, and centrifuged. Hydrogen-3 radioactivity in the combined supernatant fractions was measured by liquid scintillation counting with external quench correction. Total ^{3}H radioactivity in 1 ml of each effluent sample was measured. ^3H_2O fractions (f_{H_2O}) in effluent samples were calculated as:

$$f_{H_2O} = \frac{f_{sup} - f_r}{1 - f_r}, \quad (1)$$

where f_{sup} was equal to the quotient of supernatant and total count rates. The fractional recovery of ^{3}H-PA in supernatant (f_r), was <1%.

Description of Residue Curves as Sums of Exponential Components

The three decaying exponential components

$$\hat{y}(t) = A_1e^{-k_1t} + A_2e^{-k_2t} + A_3e^{-k_3t}, \quad (2)$$

were fitted to the residue data using a nonlinear weighted least squares fitting routine. The three terms were taken to correspond to the very rapid vascular component (A_1, k_1), and two components of clearance from tissue, a less rapid early component (A_2, k_2), and a slow, late component (A_3, k_3). Goodness of fit was evaluated by examination of residuals (differences between measured (y) and predicted ($\hat{y}$) values of data points) and by calculation of the reduced chi-squared statistic (*14*):

$$\frac{\chi^2}{\nu} = \frac{1}{\nu}\sum_{i=1}^{N}\frac{[y_i - \hat{y}_i]^2}{y_i}, \quad (3)$$

where ν is the number of degrees of freedom, that is, the total number of sample points, minus the number of parameters being estimated, minus one. If all the residuals can be accounted for by the known variances of the measured data points, the reduced chi-squared statistic has an expectation value near unity (*14*).

Description of the Compartmental Model

In principle, estimation of myocardial utilization of LCFA using an externally detectable radiolabeled LCFA requires the use of a radiokinetic model that reliably describes the major metabolic pathways available to the tracer. The level of model complexity, however, must be limited by the known properties of the identifiability of the model parameters in the available data. The model shown in Figure 1 was chosen for the fitting

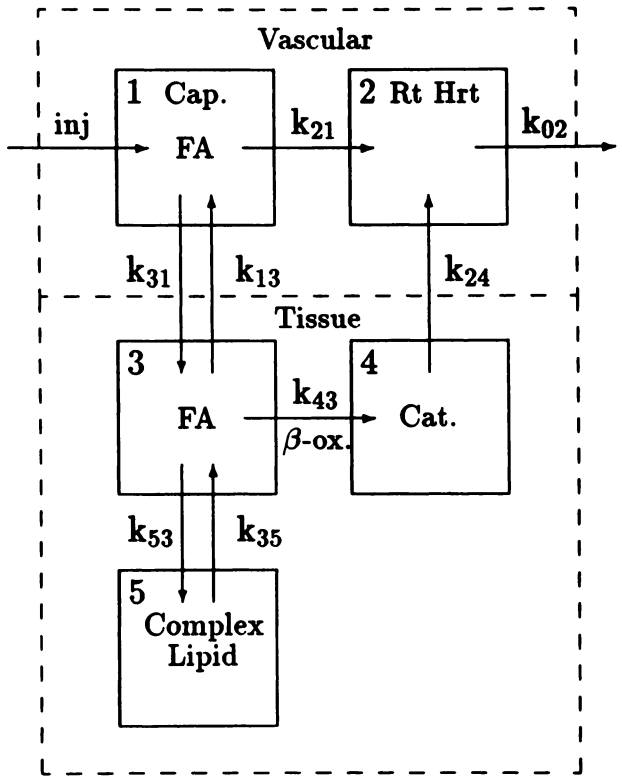

FIGURE 1
Compartmental model used to fit the tissue residues of omega-labeled LCFA in the isolated rat heart. Details of the interpretation of this greatly simplified model are provided in the text.

of the measured kinetics of omega-labeled LCFA in the isolated rat heart; this was the most complex model capable of being supported by the tissue residue data. Transfer of radioactivity between compartments is described by first order kinetics. This model is similar to the three-compartment model proposed by Huang et al. (*10*) to describe 1-^{11}C-palmitate kinetics. However, since the whole heart is in the field of view of the detectors, two additional compartments were added to account for the radioactivity in the capillary and right heart chambers. Compartment 1 represents the capillary bed in which the injected radiotracer enters the system. Labeled fatty acid is transported from the capillary bed to the right heart chambers by coronary flow. The rate constant describing this process, k_{21}, is fixed a priori at a value equal to the quotient of the average coronary flow rate and the literature value of the capillary volume of ~100 μl (*15*). Values of k_{21} were 3-5 sec^{-1} in working rat hearts. The right heart chambers are designated as Compartment 2 and are cleared with a rate constant k_{02}.

Compartment 3 represents nonesterified fatty acid in the tissue, which is assumed to have the kinetic behavior of a single compartment. Exchange of labeled fatty acid between the capillary bed and the tissue compartment is described by the rate constants k_{31} and k_{13}. The model assumes a single barrier between capillary and myocytes. There are known to be at least two barriers to fatty acid transport, including the endothelial and sarcoplasmic membranes. The single barrier model is therefore a phenomenologic reduction which is found to be sufficient to fit the data.

Compartment 4 represents labeled catabolite within tissue that is produced by beta-oxidation of the LCFA. This model assumes a single, kinetically homogenous catabolite pool within the heart. The production of catabolite from tracer is described by the rate constant k_{43}. Diffusion of catabolite from tissue is described by the rate constant k_{24} leading from the catabolite pool directly into the right heart chambers. Bypassing the capillary compartment in this way requires the assumption that the re-extraction of catabolite back into tissue can be neglected, and provides a considerable simplification of the model calculations. Conventionally, a compartment can only represent one chemical specie, but in this case, tracer and catabolite can both be contained in the right heart compartment since neither can re-enter the other compartments of the system.

In the most simplified interpretation of the model, compartment 5 would represent radiotracer incorporated into complex lipids. Exchange of tracer between free fatty acid and this compartment is described by the rate constants k_{53} and k_{35}. However, such use of a single compartment for esterified tracer is a major reduction of the model as there are known to be multiple pools of complex lipids in myocardium that are labeled by omega-labeled LCFA (*13,16*). In fact, the most valid interpretation of compartment 5 would be that it represents all labeled compounds that are not themselves substrates for beta-oxidation, but that must pass through the metabolizable compartment before leaving the heart. The interpretation of this compartment is discussed further in the Discussion section below.

The system of linear differential equations describing the mass transfer of radiolabel in the compartmental model was solved numerically (*17*). The formulation of this solution was based on that of Chu and Berman (*18*), and capitalizes on the exponential nature of the analytical solution. The numerical solution was extended to correctly represent discrete radioactive count data in the isolated rat heart. A step function of width 0.2 sec was used as the input function, consistent with the estimated duration of the bolus injections. Parameter estimation was accomplished by conventional methods based on the Marquardt algorithm (*14*). Goodness of fit was evaluated as previously described for exponential fitting.

Derivation of Indices of Fatty Acid Utilization from Compartmental Model Parameter Estimates

Indices that describe the fate of the tracer fatty acid can be derived from relationships among compartmental fluxes calculated from parameter estimates. The relative contributions of backdiffusion, of esterification followed by incorporation into complex lipids, and of oxidation to the total efflux from the nonesterified IPPA compartment were estimated in this way. According to the model, the flux of a given process is given by the product of the source compartment radioactivity and the rate constant representing the process. Therefore, the fraction of IPPA turnover resulting from backdiffusion (F_{bk}) is estimated by $k_{13}/(k_{13} + k_{43} + k_{53})$. The fractions for esterification (F_{est}) and oxidation (F_{ox}) are similarly calculated. A derivation of the steady-state oxidized fraction of IPPA (OF_{IPPA}), that is, the steady-state fraction of the total IPPA delivered to the heart by the coronary arterial flow that is oxidized, is described in the Appendix.

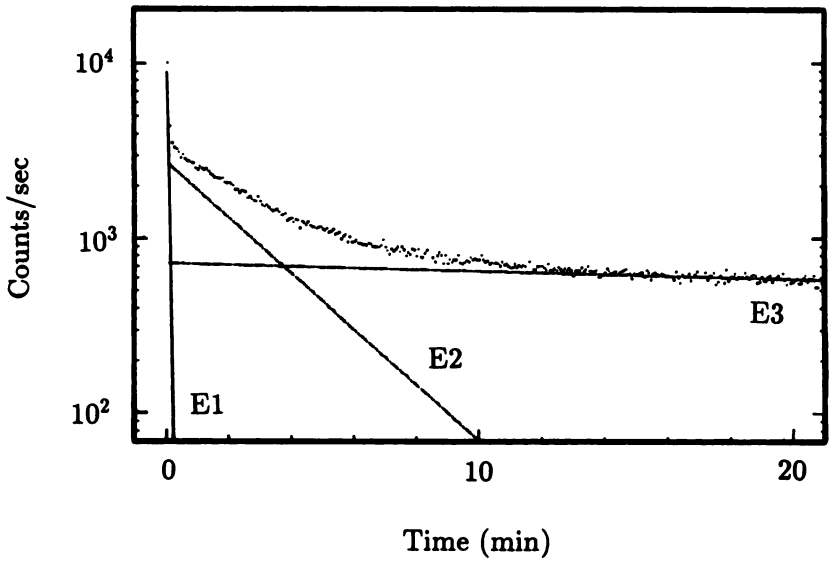

FIGURE 2
Representative [^{125}I]IPPA residue curve from a single experiment in a control heart. The data points are plotted along with the three exponential components determined by least squares fitting.

RESULTS

Exponential Fitting

^{125}IPPA residue curves were fitted with exponential components corresponding to vascular (very rapid), early (less rapid) and late (slow) clearance components. Figure 2 shows the three fitted exponential components from a representative study. Table 1 presents the average values of fitted parameter estimates. Analysis of residuals showed the failure of the fit during the first minute of data collection, that is, during the transition between vascular washout and the early tissue clearance phase. Effects of POCA on the myocardial kinetics of IPPA were clearly shown in the fitted exponential parameters values. POCA increased the early slope (k_2), decreased the late slope (k_3), and decreased the relative size of the early tissue clearance component ($A_2/(A_2 + A_3)$).

Compartmental Modeling

IPPA residue curves were more satisfactorily fitted by the compartmental model. Figure 3 shows the decomposition of the compartmental fit for the same study shown in Figure 2. Fitted values of compartmental model parameters are presented in Table 2. Values of the reduced chi-squared statistic of ~1.05 were significantly lower than those obtained by exponential fitting of the same data. Furthermore, examination of residuals showed a better fit to the early data. Determinations of myocardial extraction of IPPA using compartmental parameter estimates corresponded well with those estimated from the exponential fitting; these were reported previously to have no significant dependence on inhibition by POCA (*13*).

POCA did decrease k_{43} and increase k_{53}, indicating a decrease in IPPA oxidation and an increase in incorporation into the slowly clearing tissue component, which includes complex lipids. Decreased values of k_{35} in POCA hearts implied slower turnover of label from these pools. Rate constants k_{13} and k_{24}, representing the diffusion of IPPA and its catabolite(s) from the hearts, were not significantly influenced by POCA. Higher uncertainties of k_{13} and k_{43} estimates in control hearts reflected higher correlation of these two parameters in model fits. The added significance of compartmental fitting relative to that of exponential curve-peeling is

TABLE 1
Best-fit Parameter Estimates from Three Exponential Component Fitting of ^{125}IPPA Residue Curves

Condition	Relative size of early component $\left(\frac{A_2}{A_2 + A_3}\right)$	k_2 (min^{-1})	k_3 (min^{-1})	$\frac{\chi^2}{\nu}$
Control (n = 4)	0.728 ± 0.136	0.380 ± 0.148	0.0168 ± 0.0072	1.11 ± 0.06
POCA (n = 4)	0.340 ± 0.054†	1.43 ± 0.29†	0.0038 ± 0.0005‡	1.11 ± 0.06

* All fits performed with 34 min of data, sampling time = 1.0 sec, numerical step size = 0.1 sec.
† $p < 0.001$ versus control.
‡ $p < 0.005$ versus control.

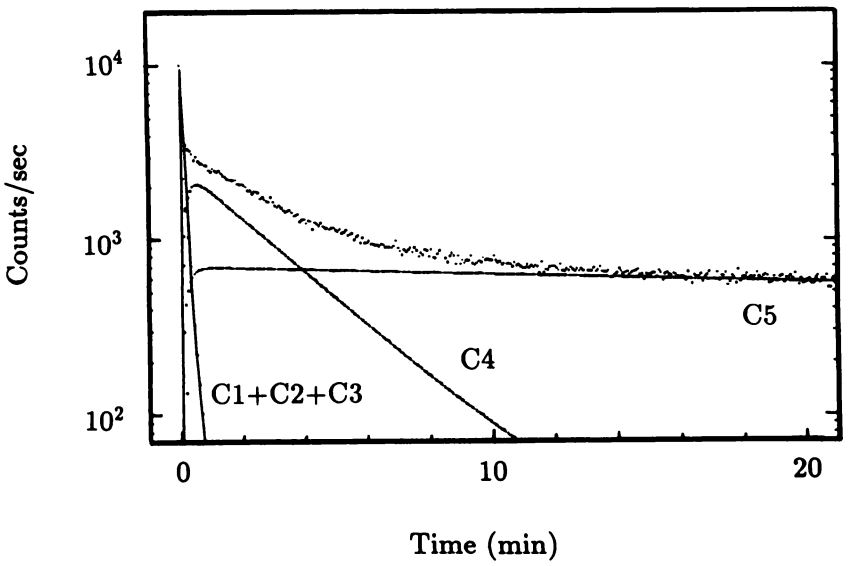

FIGURE 3
The same representative [^{125}I]IPPA residue curve as in Figure 2, shown together with the model compartmental time courses determined by nonlinear least-squares optimization of the model shown in Figure 1.

demonstrated by comparison of the values in Table 2 with those of Table 1. The estimated values of k_{13} and k_{24} were consistent with results obtained from exponential fitting for both control and inhibited hearts; however, the early slope (k_2) corresponded most closely to k_{24} (catabolite diffusion) for control hearts and k_{13} (backdiffusion of fatty acid) for POCA hearts. The late slope (k_3) corresponded well with k_{35}, the apparent turnover of the complex lipid pool, for both conditions.

Table 3 presents combinations of rate constants which express the fraction of nonesterified IPPA undergoing backdiffusion, esterification, or oxidation in control and POCA hearts. POCA caused a threefold increase in the esterified fraction, and a threefold decrease in the oxidized fraction. The fraction undergoing backdiffusion was not significantly changed. POCA effected a 70% decrease in the apparent steady-state oxidized fraction of IPPA (OF_{IPPA}) in comparison to a 90% measured inhibition of palmitate oxidation. The apparent oxidized fraction of IPPA was 1.8 times that estimated from the rate of tritiated water production from tritiated palmitate under control conditions.

Figure 4 shows simulated time courses of radioactivity in tissue and coronary effluent from parameter estimates in control and POCA hearts. The predicted percentages of catabolite in the coronary effluent were similar to those measured (*13*). The effluent catabolite curves after pre-treatment with POCA rose more slowly and fell more rapidly than did the control curves. However, predicted levels in tissue of labeled complex lipid were higher and nonesterified IPPA lower than measured levels at early times (*13*).

DISCUSSION

Early studies with [1-^{11}C]palmitic acid (CPA) (*2,3, 19*) led investigators to regard the early slope of labeled LCFA residue curves as an index of LCFA oxidation. However, more recent results in ischemic hearts (*6,7*) have revealed limitations of this interpretation due to the confounding influence of backdiffusion of extracted but unoxidized CPA in the early clearance kinetics. Because the diffusion rates of $^{11}CO_2$ and CPA are both rapid, the contribution of catabolite and tracer to the early washout cannot be discriminated from residue curves alone. Therefore, the relative size and slope of the early clearance phase may not be reliable indices of LCFA oxidation in all conditions (*1*). Omega-labeled LCFA may have an advantage over CPA for in vivo studies of LCFA utilization if the diffusion rate of a labeled catabolite is sufficiently different from the back-

TABLE 2
Best-fit Model Parameter Estimates from Compartmental Model Fitting of ^{125}IPPA Residue Curves*

Condition	k_{13} (min^{-1})	k_{43} (min^{-1})	k_{53} (min^{-1})	k_{24} (min^{-1})	k_{35} (min^{-1})	$\frac{\chi^2}{\nu}$†
Control (n = 4)	2.1 ± 1.9	2.0 ± 1.4	0.89 ± 0.69	0.32 ± 0.16	0.017 ± 0.011	1.06 ± 0.03
POCA (n = 4)	2.1 ± 0.1	0.39 ± 0.14‡	2.31 ± 0.49‡	0.46 ± 0.16	0.0067 ± 0.0008‡	1.04 ± 0.033

* Fits were performed with 34 min of data, sampling time = 1.0 sec, numerical step size = 0.1 sec.
† Reduced chi-squared statistic.
‡ $p < 0.01$ versus control.

TABLE 3
Indices of ^{125}IPPA Kinetics Derived from Compartmental Model Parameter Estimates

Index	Expression	Interpretation	Control (n = 4)	POCA treated (n = 4)	Significance
F_{bk}	$\frac{k_{13}}{k_{13}+k_{43}+k_{53}}$	Fraction of IPPA turnover resulting from back diffusion	0.465 ± 0.198	0.413 ± 0.039	N.S.
F_{est}	$\frac{k_{53}}{k_{13}+k_{43}+k_{53}}$	Fraction of IPPA turnover resulting from esterification	0.164 ± 0.078	0.471 ± 0.075	$p < 0.001$
F_{ox}	$\frac{k_{43}}{k_{13}+k_{43}+k_{53}}$	Fraction of IPPA turnover resulting from oxidation	0.371 ± 0.150	0.116 ± 0.053	$p < 0.001$
OF_{IPPA}	$\frac{k_{31}k_{43}}{[(k_{21}+k_{31})(k_{43}+k_{53})+k_{21}k_{13}]}$	Steady-state oxidized fraction	0.088 ± 0.041	0.030 ± 0.021	$p < 0.01$

diffusion rate of the unoxidized tracer that these two processes can be kinetically discriminated using a compartmental modeling technique.

Schön et al. investigated the radiokinetics of CPA (*2*) and ^{123}I-17-iodoheptadecanoic acid (IHPA) (*8*) in an open-chest dog model. Unlike that of CPA, the clearance half-time of the early phase for IHPA increased with myocardial oxygen consumption, suggesting that increased LCFA oxidation slowed ^{123}I clearance. However, the ratio between the size of the early and late phases correlated positively with myocardial oxygen consumption. Our IPPA data are consistent with these findings, showing greater relative size and lesser slope of the early clearance component for control hearts compared to those with impaired LCFA oxidation (Table 1).

Although results such as these with omega-iodoalkyl and omega-iodophenol fatty acids may at first appear uninterpretable, they are explained in terms of the slower diffusion rates of the catabolite(s) produced upon beta-oxidation of these radioanalogs in myocardium. In isolated hearts perfused without albumin, clearance kinetics of omega-iodoalkyl fatty acids are rate-limited by diffusion of radioiodide (*13,20,21*). In our present data, characteristic diffusion rates of IPPA catabolites appeared to be four or more times slower than those of

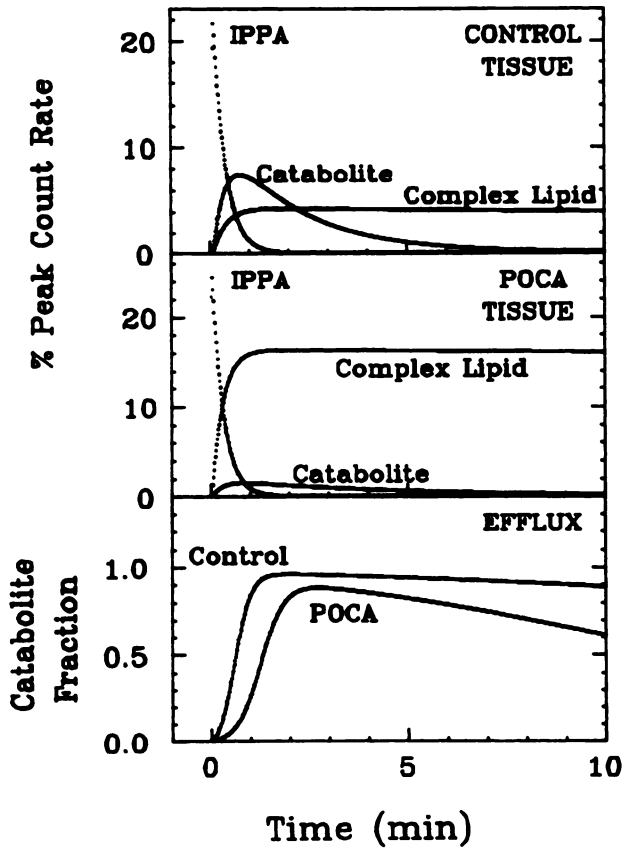

FIGURE 4
Model predictions of tissue and effluent time courses following bolus injections of [^{125}I]IPPA. The curves were calculated using the model shown in Figure 1 and the averaged fitted rate constants for the control and POCA conditions listed in Table 2. The identities of the curves in the upper two panels correspond to those of the model curves plotted in Figure 3. The fitted parameters are clearly consistent with a sharp depression of catabolite production, and increased incorporation into a slowly clearing, nonmetabolizable compartment. The bottom panel shows that the fraction of the coronary effluent radioactivity attributable to catabolite is predicted to rise more slowly, and decline from its maximum value, in hearts inhibited by POCA, in good agreement with measurement.

the unoxidized tracer in hearts perfused with albumin. The behavior of the early clearance component in IPPA residue curves was thus very sensitive to the relative contributions of IPPA and catabolite(s) to the early washout. For control hearts, the early slope reflected primarily the clearance of catabolite(s), that is slower than that of IPPA. The contribution of backdiffusion of IPPA to early clearance was enhanced by the inhibition of LCFA oxidation by POCA, thus increasing the early slope. The decrease of the relative size of the early component with POCA was consistent with decreases of oxidation and concomitant increases in esterification of IPPA predicted by compartmental modeling.

It is important to note that increased incorporation of IPPA into complex lipids implied by the model fits cannot in fact account for the increased size of the late component observed with POCA. Analysis of tissue radioactivity showed that only ~5% of the radiolabel in hearts was associated with complex lipids at 1 min postinjection (*13*). The majority of label was nonesterified IPPA. This implies the existence of a nonesterified IPPA pool kinetically distinct from the pool available for backdiffusion. The following are three possible explanations for this result.

1. The retained fraction reflects intracellular IPPA, while the transient pool is associated with the endothelial and interstitial spaces. Backdiffusion of IPPA from myocytes is minimal in this case.
2. An additional intracellular pool may be utilized for oxidation or lipid synthesis but is not readily available for diffusion from the cell.
3. The retained IPPA pool is utilized for lipid synthesis but not readily available for oxidation.

These suggestions are consistent with what is known about the compartmentation of NEFA and the involvement of fatty acid binding proteins in LCFA transport and regulation of beta-oxidative activity (*22*). However, for the purposes of parameter estimation, the additional model complexity implied by these suggestions could not be supported by the residue data. Rapid turnover of compartment 3 (nonesterified IPPA) adequately accounts for the early backdiffusion kinetics. Therefore, the implied additional IPPA pool is apparently combined with complex lipid in the compartmental model fits. Further work is required to fully characterize this fraction and to validate the ability of the model to predict LCFA oxidation in spite of this model inadequacy.

In conclusion, our results demonstrate that compartmental modeling allows the contributions of tracer and catabolite diffusion to the early residue data to be estimated as long as the diffusion rate constants for these two processes are kinetically distinct. Modified omega-labeled LCFA may thus have an advantage over radiocarbon labeled unmodified LCFAs. In addition, our work may be useful in the development of radiotracers and operational equations for estimation of the rate of beta-oxidation of LCFA in vivo using positron tomography. Additional considerations would have to be addressed for in vivo modeling, including the influences of heterogeneity of perfusion, heterogeneity of plasma fatty acids, temporal distribution of the input function, systemic recirculation of metabolites, and longer scan times on the applicability of the compartmental modeling technique.

APPENDIX

Derivation of Steady-State Indices of LCFA Utilization

In general, a metabolic rate is estimated in a radiotracer technique as the product of its steady-state precursor pool concentration (or radioactivity) and the rate constant describing the formation of product. Thus, the oxidative rate of palmitate is estimated by the steady-state production of labeled catabolites from IPPA in the heart (CPR):

$$\text{CPR}(\mu\text{Ci/min/heart}) = k_{43}C_3, \qquad \text{(A.1)}$$

where C_3 (μCi/heart) is the steady-state radioactivity of the nonesterified IPPA compartment, or compartment 3. In bolus injection studies, the system never reaches steady-state with respect to compartmental quantities of radiolabeled species. Therefore, the value of C_3 must be evaluated from the dynamically estimated rate constants as determined by the steady-state solution of the mass-balance equations. In good analogy with the expressions used for estimation of the phosphorylation rate of deoxyglucose (*23*), the steady-state solution of the kinetic equations was derived using the assumption that the incorporation of label into the slowly clearing compartment 5 was in fact irreversible. In the true steady state, incorporation into compartment 5 would be exactly matched by label returning from compartment 5 to compartment 3; the presence of compartment 5 would thus have no influence on the steady-state concentration in compartment 3. However, this true steady-state condition would occur only after tens of hours, analogous to the comparable times required to reach the steady state of deoxyglucose-6-phosphate. For analysis of data measured in the first hour after administration of tracer, the steady-state solution can be accurately approximated by neglecting the return of tracer from complex lipid. In this case, k_{35} is set to zero and solution of the mass-balance equations for the steady-state quantity of nonesterified IPPA becomes

$$C_3 = \frac{k_{31}\dot{x}_{33}}{[(k_{21} + k_{31})(k_{43} + k_{53}) + k_{21}k_{13}]}, \qquad \text{(A.2)}$$

where $\dot{x}_{33}$ (μCi/heart/min) is the steady-state input of radiotracer to the system. For a constant infusion of perfusion medium containing the radiotracer in concentration C_{IPPA}, the input rate is

$$\dot{x}_{33} = F_c C_{IPPA}. \qquad \text{(A.3)}$$

Combinding Equations (A.1), (A.2), and (A.3), the catabolite

production rate becomes

$$\text{CPR}(\mu\text{Ci/min/heart}) = \frac{k_{31}k_{43}F_c C_{IPPA}}{[(k_{21} + k_{31})(k_{43} + k_{53}) + k_{21}k_{13}]}, \quad \text{(A.4)}$$

or

$$\text{CPR}(\mu\text{Ci/min/heart}) = F_c C_{IPPA} OF_{IPPA}, \quad \text{(A.5)}$$

where OF_{IPPA} is the steady-state oxidized fraction of IPPA and is therefore calculated as

$$OF_{IPPA} = \frac{k_{31}k_{43}}{[(k_{21} + k_{31})(k_{43} + k_{53}) + k_{21}k_{13}]}. \quad \text{(A.6)}$$

ACKNOWLEDGMENTS

This work was supported by National Heart, Lung and Blood Institute awards RO1-HL36534 and HL29046.

REFERENCES

1. Schelbert HR, Schwaiger M. PET studies of the heart. In: Phelps ME, Mazziotta JC, Schelbert HR, eds. *Positron emission tomography and autoradiography. Principles and applications for the brain and heart.* New York: Raven Press, 1986:581–661.
2. Schön HR, Schelbert HR, Robinson G, et al. C-11 labeled palmitic acid for the noninvasive evaluation of regional myocardial fatty acid metabolism with positron-computed tomography. I. Kinetics of C-11 palmitic acid in normal myocardium. *Am Heart J* 1982; 103:532–547.
3. Schön HR, Schelbert HR, Robinson G, Kuhl DE, Phelps ME. C-11 labeled palmitic acid for the noninvasive evaluation of regional myocardial fatty acid metabolism with positron-computed tomography. II. Kinetics of C-11 palmitic acid in acutely ischemic myocardium. *Am Heart J* 1982; 103:548–561.
4. Machulla HJ, Stöcklin G, Kupfernagel C, et al. Comparative evaluation of fatty acids labeled with C-11, C1-34m, Br-77, and I-123 for metabolic studies of the myocardium. *J Nucl Med* 1978; 19:298–302.
5. Reske SN, Schön S, Schmitt W, Machulla HJ, Knopp R, Winkler C. Effect of myocardial perfusion and metabolic interventions on cardiac kinetics of phenylpentadecanoic acid (IPPA) I-123. *Eur J Nucl Med* 1987; 12:S27–S31.
6. Fox KAA, Abendschein DR, Dieter Ambos H, Sobel BE, Bergmann SE. Efflux of metabolized and nonmetabolized fatty acid from canine myocardium. Implications for quantifying myocardial metabolism tomographically. *Circ Res* 1985; 57:232–243.
7. Rosamond TL, Abendschein DR, Sobel BE, Bergmann SR, Fox KAA. Metabolic fate of radiolabeled palmitate in ischemic canine myocardium: implications for positron emission tomography. *J Nucl Med* 1987; 28:1322–1329.
8. Schön HR, Senekowitsch R, Berg D, et al. Measurement of myocardial fatty acid metabolism: Kinetics of I-123 heptadecanoic acid in normal dog hearts. *J Nucl Med* 1986; 28:1449–1455.
9. Schön HR. I-123 heptadecanoic acid-value and limitations in comparison with C-11 palmitate. *Eur J Nucl Med* 1986; 12:S16–S19.
10. Huang SC, Schwaiger M, Selin C, Phelps ME, Schelbert HR. Tracer kinetic model of C-11 palmitate (CPA) for estimating regional free fatty acid utilization in myocardium [Abstract]. *J Nucl Med* 1984; 24:P12.
11. Dubois F, Depresseux JC, Bontemps L, et al. Mathematical model of the metabolism of ^{123}I-16-iodo-9-hexadecenoic acid in an isolated rat heart. Validation by comparison with experimental measurements. *Eur J Nucl Med* 1986; 11:453–458.
12. Bontemps L, Demaison L, Dubois F, et al. A new experimental model for studies of drug actions on myocardial metabolism. Application to a study of the influence of POCA. *Nucl Med Biol (Int J Radiat Appl Instrum B)* 1987; 14:459–465.
13. DeGrado TR, Holden JE, Ng CK, Raffel DM, Gatley SJ. Comparison of 16-iodohexadecanoic acid (IHDA) and 15-p-iodophenylpentadecanoic acid (IPPA) metabolism and kinetics in the isolated rat heart. *Eur J Nucl Med* 1988; 14:600–606.
14. Bevington PR. Data reduction and error analysis for the physical sciences. New York: McGraw-Hill, 1969:187–203.
15. Bassingthwaighte JB, Winkle B. Kinetics of blood to cell uptake of radiotracers. In: Colombetti LG, ed. *Biological transport of radiotracers.* Boca Raton, FL: CRC Press, 1982:97–146.
16. Reske SN, Sauer W, Machulla HJ, Winkler C. 15(p-[^{123}I]Iodophenyl)pentadecanoic acid as tracer of lipid metabolism: comparison with [1-^{14}C]palmitic acid in murine tissues. *J Nucl Med* 1984; 25:1335–1342.
17. Halama JR. Tracer kinetic studies of glucose transport and metabolism using ^{18}F-fluorosugars in isolated rat hearts. PhD thesis, University of Wisconsin-Madison, 1983.
18. Chu SC, Berman M. An exponential method for the solution of systems of ordinary differential equations. *Commun ACM* 1974; 17:699–702.
19. Goldstein RA, Klein MS, Welch MJ, Sobel BE. External assessment of myocardial metabolism with C-11 palmitate in vivo. *J Nucl Med* 1980; 21:342–348.
20. Kloster G, Stöcklin G. Determination of the rate-determining step in halofatty acid turnover in the heart. *Radioakt Isotope Klin Forsch* 1982; 15:235–241.
21. Reske SN, Auner G, Winkler C. Kinetics of 17-(^{123}I) iodoheptadecanoic acid in myocardium of rats. *J Radioanal Chem* 1983; 79:355–361.
22. Fournier NC. Uptake and transport of lipid substrates in the heart. *Basic Res Cardiol* 1987; 82(suppl 1):11–18.
23. Phelps ME, Hoffman EJ, Selin C, Sokoloff L, Kuhl DE. Tomographic measurement of local cerebral metabolic rate in humans with (F-18) 2-fluoro-2-deoxy-D-glucose: validation of method. *Ann Neurol* 1979; 6:371–388.